Fast volumetric imaging of ethanol metabolism in rat with hyperpolarized [1-^{13}C]-pyruvate

S. Josan[1,2], D. Spielman[2], Y-F. Yen[3], R. Hurd[3], A. Pfefferbaum[1,4], and D. Mayer[1,2]
[1]SRI International, Menlo Park, CA, United States, [2]Radiology, Stanford University, Stanford, CA, United States, [3]GE Healthcare Applied Science Laboratory, Menlo Park, CA, United States, [4]Psychiatry and Behavioral Sciences, Stanford University, Stanford, CA, United States

Introduction

Rapid, time-resolved, volumetric imaging of hyperpolarized pyruvate (Pyr) and its metabolic products lactate (Lac) and alanine (Ala) allows the measurement of metabolic activity in different tissues and can be useful to distinguish between normal and diseased tissues. This work applies dynamic 3D magnetic resonance spectroscopic imaging (MRSI) to investigate Pyr metabolism modulated by ethanol.

Ethanol is metabolized in the liver via the breakdown of ethanol to acetaldehyde and acetaldehyde to acetate. Both of these reactions reduce the coenzyme nicotinamide adenine dinucleotide (NAD+) to NADH. Thus, ethanol consumption leads to accumulation of NADH in the liver. Because NADH is also a coenzyme in Pyr-to-Lac conversion, this altered liver metabolic state created by ethanol can be interrogated by hyperpolarized Pyr measurements.

Spielman et al [1] have previously reported MRS measurements of hyperpolarized Pyr to study rat liver metabolism modulated by ethanol. Dynamic ^{13}C MRS was used to measure the conversion rates of Pyr to Lac and Ala in the presence and absence of ethanol. However, the MRS data were not spatially localized within a slice, which contained vascular and other structures in addition to the targeted organs. Dynamic 3D ^{13}C MRSI can provide improved rate-constant estimates by allowing the analysis of spectra from organ-specific regions-of-interest (ROIs). This work extends the 2D spiral MRSI sequence [2] to provide volumetric coverage and applies it to ethanol metabolism.

Methods

All measurements were performed on a GE 3T MR scanner equipped with self-shielded gradients (40 mT/m, 150 mT/m/ms). A custom-built dual-tuned (^{1}H/^{13}C) quadrature coil (dia=80 mm, length=90 mm) was used for RF excitation and signal reception. Healthy male Wistar rats (275-315 g weight, n=3) were injected in a tail vein with 3 ml of 80-mM solution of [1-^{13}C]-pyruvate that was hyperpolarized via Dynamic Nuclear Polarization (22-26% liquid state polarization). The time from dissolution to start of injection was 24s.

The 2D undersampled spiral spectroscopic imaging sequence described in [2] was extended for volumetric coverage. A spiral readout trajectory encoded the spectral and two spatial (x-y) dimensions. The slice (z) direction used 12 phase encoding steps in a centric order. Imaging parameters were: FOV=80×80×60 mm^3, 5×5×5 mm^3 nominal resolution, spectral width=280 Hz, 42mm slab excitation, 36 excitations/volume, flip angle=5.6º, TE=3ms, total acquisition time=4.5 s. Dynamic ^{13}C MRSI data were acquired from a 3D volume that included both liver and kidney every 5 s for 80 s, starting at the same time as the Pyr injection.

After acquiring a baseline ^{13}C MRSI measurement, 1.0 g/kg of a 20% ethanol solution was injected into the tail vein at the rate of 1 ml/min. Another ^{13}C MRSI measurement was acquired approximately 45 min after ethanol injection to achieve a targeted steady-state blood alcohol level (BAL) of 100 mg/dL at the time of the second acquisition. At the end of the exam, blood was collected for BAL analysis.

The data were reconstructed similar to the 2D case described in [2] with an additional Fourier transform step for the slice direction. The data were zero-filled by a factor of 2 in each direction. Metabolic maps for Pyr, Lac, and Ala were calculated by integrating the signal within ±20 Hz around each peak in absorption mode. ROIs were drawn manually for liver, kidney and vasculature in the corresponding slices to calculate the time-resolved signal intensities for Pyr, Lac and Ala. These metabolite time-courses were then fit using a three-site exchange model to estimate the Pyr-to-Lac (k_{pl}) and Pyr-to-Ala (k_{pa}) rate constants. The same model was used as in [1] except that the measured Pyr time-course was used as the bolus input into the model.

Results and Discussion

Figure 1 shows representative ^{13}C metabolic maps of Pyr, Lac and Ala superimposed on ^{1}H 3D SPGR images. Figure 2 plots the time courses from an ROI in the liver, and the corresponding fits, for one subject. The estimated apparent k_{pl} and k_{pa} rate constants for 3 subjects are summarized in Table1. The BAL values ranged between 82.8-101.6 mg/dL. The average apparent liver k_{pl} increased from 0.050 ± 0.005 s^{-1} pre-ethanol to 0.071 ± 0.009 s^{-1} post-ethanol, confirming the hypothesis that NADH levels are rate-limiting for liver Pyr-to-Lac conversion [1]. A smaller increase in apparent k_{pl} was observed in the kidney compared to the liver due to lower levels of alcohol dehydrogenase [1]. As a control, apparent k_{pa} measured simultaneously in liver, kidney and vasculature ROIs, as well as vasculature k_{pl} showed no significant change. Compared to the slice-selective MRS measurements in [1], the organ specific k_{pl} and k_{pa} values obtained here were higher in the liver but similar in the kidney, since the fraction of Pyr signal contribution from the blood is much higher for the liver slice than for kidney.

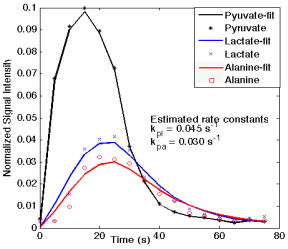

Figure2: Liver time-course data, curve fits, and calculated rate constants

This work demonstrates time-resolved volumetric metabolic imaging of hyperpolarized ^{13}C Pyr and its metabolic products using an undersampled spiral CSI sequence, with an acquisition time of 4.5 s for a nominal 5mm isotropic resolution. The dynamic 3D acquisition allows the analysis of spectra from organ-specific ROIs, thus providing improved rate-constant estimates.

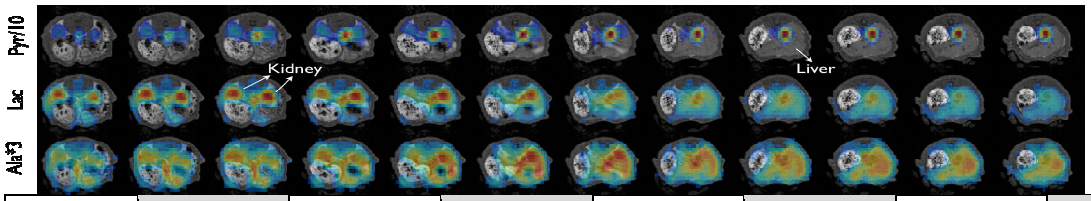

Figure 1: Representative Pyr, Lac and Ala images superimposed on ^{1}H MRI slices from the 3D volume covering kidneys and liver. ^{13}C images are averaged over all 16 time-points acquired.

	Liver Kpl (s^{-1})	Liver Kpa (s^{-1})	Kidney Kpl (s^{-1})	Kidney Kpa (s^{-1})	Liver vasc. Kpl (s^{-1})	Liver vasc. Kpa (s^{-1})	Kidney vasc. Kpl (s^{-1})	Kidney vasc. Kpa (s^{-1})
pre-ethanol	0.050 ± 0.005	0.029 ± 0.004	0.016 ± 0.004	0.005 ± 0.002	0.005 ± 0.002	0.002 ± 0.0	0.007 ± 0.003	0.004 ± 0.002
post-ethanol	0.071 ± 0.009	0.030 ± 0.009	0.019 ± 0.003	0.005 ± 0.001	0.005 ± 0.002	0.002 ± 0.001	0.007 ± 0.003	0.003 ± 0.001
% change	42.1 ± 23.4	0.9 ± 18.9	17.3 ± 6.7	-4.8 ± 8.3	11.1 ± 19.3	-16.7 ± 28.9	-1.2 ± 26.8	-23.3 ± 25.2

References: [1] Spielman D *et al* [2009], MRM 62:307:313, [2] Mayer D *et al* [2009], MRM 62:557:564,
Acknowledgements: NIH grants RR09784, AA05965, AA018681, AA13521-INIA, and EB009070